

후 확산 공정 변수가  $p^+$  실리콘 박막의 잔류 응력 분포에 미치는 영향정 옥 찬, 양 상 식  
아주대학교 전자공학부Effects of Drive-in Process Parameters on the Residual Stress Profile of the  $p^+$  Silicon FilmOk Chan Jeong, Sang Sik Yang  
School of Electronics Eng., Ajou University

**Abstract** - The paper represents the effects of the drive-in process parameters on the residual stress profile of the  $p^+$  silicon film. For the quantitative determination of the residual stress profiles, the test samples are doped via the fixed boron diffusion process and four types of the thermal oxidation processes and consecutively etched by the improved process. The residual stress measurement structures with the different thickness are simultaneously fabricated on the same silicon wafer. Since the residual stress profile is not uniform along the direction normal to the surface, the residual stress is assumed to be a polynomial function of the depth. All of the coefficients of the polynomial are determined from the deflections of cantilevers and the displacement of a rotating beam structure. As the drive-in temperature or the drive-in time increases, the boron concentration decreases and the magnitude of the average residual tensile stress decreases. Also, near the surface of the  $p^+$  film the residual tensile stress is transformed into the residual compressive stress and its magnitude increases.

**Quantitative Analysis Method**

The quantitative measurement method of the residual stress in  $p^+$  silicon film were suggested by Yang et al[1, 2]. Several cantilever structures and a rotating beam structure are used to find the relative stress profile and the average stress, respectively. Figure 1 illustrates two profiles obtained for two cases of different drive-in processes. Type A has a larger stress in the tensile region and a steeper gradient near the surface than Type B. Because the boron diffusion process conditions and the drive-in process conditions of two examples are different from each other, it is impossible to investigate that the effect of two-step diffusion process parameters on the residual stress profile. In addition, the possibility of the error occurrence in the determination of the residual stress is very large since the test structures for the residual stress analysis are designed and fabricated on different silicon wafers. Therefore, an improved study on the effect of the drive-in process parameters is needed.

For the systematic research on the quantitative determination of the residual stress profile for the analysis of the effect of the drive-in process parameters, the polynomial function in Ref. [1] is revised, and the modified method to fabricate test structures is suggested. Also, the lattice constant variations of the boron-doped silicon wafer with the various dopant levels are measured by HRXRD as the nondestructive method. Moreover, the correlation coefficients between the boron concentration and the residual stress are calculated and discussed.

**Revision of Quantitative Analysis Method**

For the calculation of the relative residual stress, equations of Ref. [1] are used. Especially, the second term in the brackets of Eq. (3) in Ref. [4] is corrected to  $\delta a_2$  and the revised residual stress profiles in Ref. [1-2] are illustrated in Figure 1. The revised residual stress profiles were estimated

by using the second-order polynomial and shifted by the thermal oxide thickness for the residual stress calculation under the original film depth. Compared with Ref. [1], the region of the compressive residual stress at the front side does not exist when the second-order polynomial is applied to Type A. In the case of Type B, the revised stress profile is quite different from the previous work.

**Test Structures Fabrication Process**

Figure 2 illustrates the improved etch process for the fabrication of the cantilevers with different thickness. The dashed-line and the solid-line represents the initial silicon state before the etch process and the silicon state after the step-by-step etch process, respectively. If each of the thermal oxide of the cantilevers, A, B, C, D, E on the same specimen are subsequently removed and etched, the cantilevers with various thicknesses can be simply fabricated. Hence, the front side of the cantilever, A is etched for ( $t_A + t_B + t_C + t_D$ ) and in the case of the cantilever, C, the etch time is ( $t_C + t_D$ ).

For the fabrication of test structures,  $n$ -type, (100) double-side polished silicon wafers are used. The boron predeposition with a solid source at 1100 °C in N<sub>2</sub> ambient gas is performed for 10 hours. The silicon wafers of the drive-in temperature are 1000 °C and 1100 °C, respectively. And, those of thermal oxidation time are 60 minutes and 90 minutes, respectively. And, the backside of the silicon wafer is etched with EPW etchant for 230 minutes. By means of the sequential oxide etch process of Fig. 3, the backsides of cantilevers are exposed to the anisotropic etchant for the various etch times. The frontside of the rotating beam and the cantilever E are protected with the thermal oxide until all processes are finished. The fabricated the rotating beam structure and the cantilevers are shown in Figure 3.

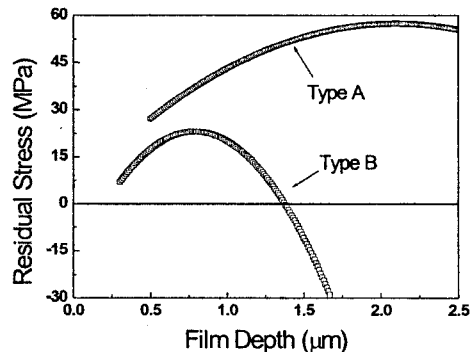


Figure 1. The revised residual stress profiles in Ref. [5].

### Determination of Residual Stress

The vertical deflections of cantilevers and the displacement of a rotating beam are measured with a surface profiler meter and by means of focusing a calibrated microscope. The displacements of the rotating beam for the average stress are compared with the FEM simulation results in Ref. [2].

Figure 4 illustrates the determined residual stress profile after the drive-in process. The front side of the boron doped silicon layer is oxidized by the drive-in process using the thermal oxidation process and this oxidized layer is removed after the final structure etch. As the drive-in time and temperature increase, the residual stress are reduced at the whole film depth and the status of the residual stress are changed from tensile to compressive and the magnitude of the residual stress increases at the region near the surface of the  $p^+$  silicon film. Table 1 illustrates the sensitivity of the average and maximum stress to film thickness, which is calculated from the difference between film thickness and the stress variation. Either when the drive-in process time increases at the low temperature, or when the drive-in temperature increases at the short process time, the average and the maximum stress are reduced much larger than the other cases.

Figure 5 shows the estimation errors in terms of each measurement errors with respect to the maximum residual stress of Type I. The determination error of the calculated residual stress profile is attributed to the inaccuracy in the measurement errors such as the vertical deflections, the thickness of the cantilevers, and the rotating measurement error. The estimation errors are defined as each errors caused by the measurement errors is divided by the maximum residual stress. The estimation errors have the different values along the film depth, and the maximum error are occurred at both ends of the film thickness. The total error in the determination of the residual stress is estimated to be about  $\pm 3\%$  of the maximum residual stress.

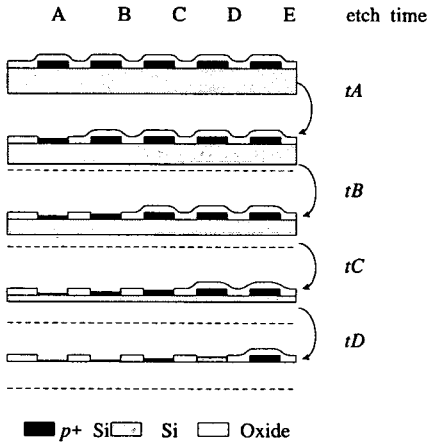


Figure 2. The etch process of the structures with the various film thickness.

Table 1. The sensitivity of residual stress to film thickness  
( $a$  : average,  $m$  : maximum, unit:  $\text{MPa}/\mu\text{m}$ )

	Time effect		Temp. effect	
	1000 °C	1100 °C	60 min	90 min
$S_a$	100	35	50	28
$S_m$	105	49	51	31

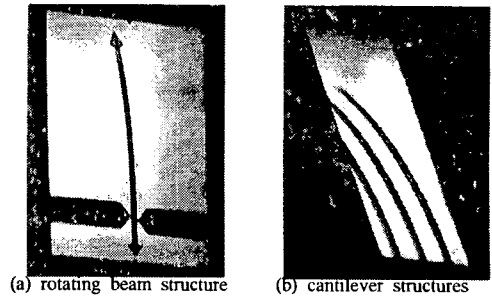


Figure 3. The residual stress profile before the drive-in process.

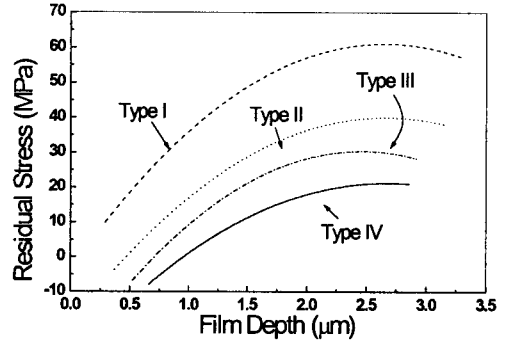


Figure 4. The residual stress profile before the drive-in process.

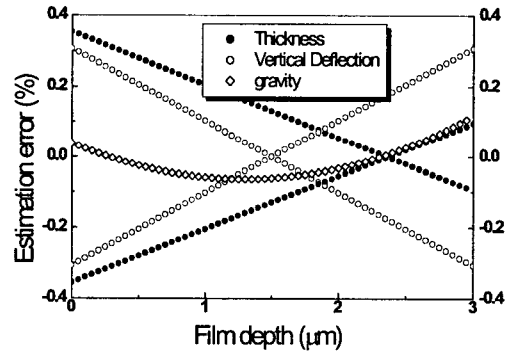


Figure 5. The estimation errors due to the measurement errors of the cantilever structure.

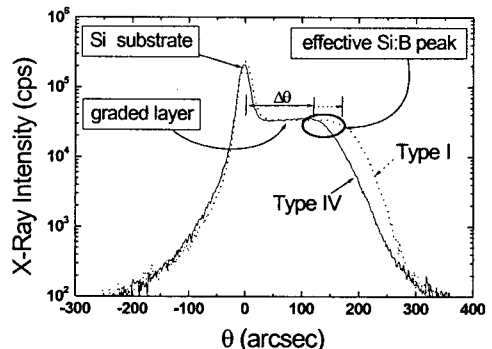


Figure 6. The rocking curves of the test wafers.

Table 2. The calculation results of the lattice contraction.

	Type I	Type II	Type III	Type IV
$a_{Si:B}$	5.3977 $\mu$	5.4016 $\mu$	5.4026 $\mu$	5.4036 $\mu$
$\Delta a/a$ (%)	-0.557%	-0.485%	-0.467%	-0.449%

Table 3. The calculated correlation coefficients.

	$C_{BA}(x) \leftrightarrow \sigma'(x)$	$C_A(x) \leftrightarrow \sigma(x)$
Type I	0.753	0.641
Type II	0.804	0.762
Type II	0.939	0.871
Type IV	0.968	0.919

- $C_{BA}(x)$  : the boron concentration difference
- $\sigma'(x)$  : the first order derivative of stress profile
- $C_A(x)$  : the boron concentration profile after drive-in

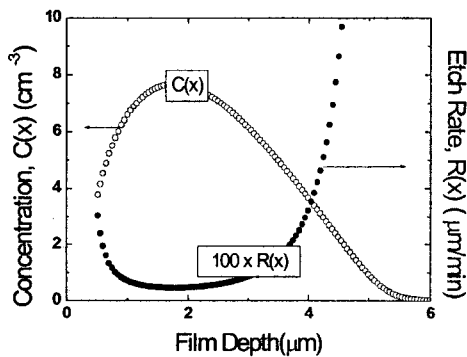


Figure 7. The estimated etch rate of Type III.

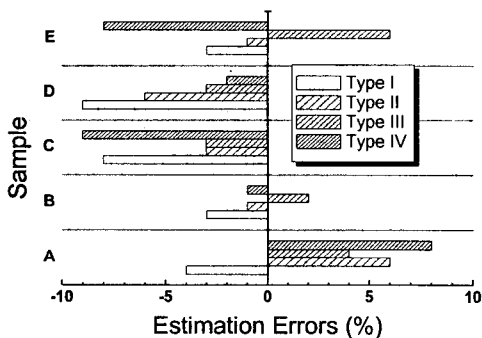


Figure 8. The estimation errors of the  $p^+$  silicon film thickness.

#### Lattice constant measurement

Figure 6 illustrates the example of the rocking curve for the boron doped test wafer measured with HRXRD (D8 Discover, Bruker AXS Inc.). The rocking curve indicates that the peak patterns are divided into three regions such as the silicon substrate, the graded lattice constant layer, the effective Si:B peak. The drive-in process time and temperature increase, the amount of decreases. Generally, the silicon substrate peak is only observed on the pattern of the undoped silicon. However, the grade layer and the effective Si:B peak are measured because of the heavily boron diffusion process[6]. Moreover, the  $p^+$  layer fabricated by the long time drive-in process shows the flat graded lattice layer and the insignificant effective Si:B peak.

The lattice contraction of the  $p^+$  silicon have been calculated by Bragg's law[7], the results of those are shown in

Table 2. The contraction ratio of Type I is the largest among the four cases. The boron atoms contract the lattice constant of the boron-doped silicon. The lattice contraction of the boron-doped silicon results in the average tensile stress of test sample. Table 2 confirms that the average stress of the measurement results and the residual stress profiles of Figure 4 are reasonable.

#### Correlation Coefficients

For the analysis of the effect of the drive-in process on the residual stress, the correlation coefficients between the boron concentration profiles and the residual stress profiles of Figure 8 are calculated. Table 4 illustrates the correlation coefficients between the boron concentration profile and the residual stress profile for each type. As the drive-in time or temperature increases, the correlation coefficient becomes close to 1. The correlation between the boron concentration variation by the drive-in process and the derivative of the stress profile is larger than that between the boron concentration after the drive-in process and the stress profile.

#### Estimation of Film Thickness

Figure 7 shows an example of the calculated etch rate of Type III by using Seidels empirical formula [8]. The boron concentration profiles simulated by T-SUPREM are used for the etch rate calculation. The critical concentration and  $a$  are set to  $2.7 \times 10^{19} \text{ cm}^{-3}$  and 1, respectively. The etch rate of the moderately doped silicon,  $R_i$  is  $1.25 \mu\text{m}/\text{min}$ . Figure 8 shows the estimation errors compared with the film thickness in the measurement results. The errors of the estimation are less than  $\pm 9\%$ .

#### Conclusions

In this paper, the rotating beam and the cantilevers with the different thickness were fabricated by an improved etch process method, and the residual stress profile was determined in the second order polynomial from the deformation of these structures. As the drive-in temperature and/or time increases, the boron concentration, the film thickness, and the average residual stress decrease. Moreover, the status of the residual stress changes from tensile to compressive near the surface of the  $p^+$  silicon layer. From the calculation results of the correlation coefficients, the residual stress profile has a close relation with the simulated boron concentration. Also, The lattice contraction of the boron-doped silicon wafer was measured with HRXRD. The residual strain caused by the boron doping process was calculated and the effect of the drive-in process was confirmed.

#### Reference

- [1] E. H. Yang, S. S. Yang, and S. H. Yoo, "A Technique for Quantitative Determination of the Profile of the Residual Stress along the Depth of  $p^+$  silicon Films," *Appl. Phys. Lett.*, Vol. 67, No. 7, pp. 912-914, 1995.
- [2] E. H. Yang, and S. S. Yang, "The Quantitative Determination of the Residual Stress Profile in Oxidized  $p^+$  Silicon Films," *Sensors and Actuators A* 54, pp. 684-689, 1996.
- [3] Wu, Kenneth Chu-Chao, "Novel Etch-Stop Materials for Silicon Micromachining," Masters of Science Thesis, MIT, Cambridge, MA. 1997. (Supervisor : Eugene A. Fitzgerald)
- [4] C. S. Lee, J. H. Lee, C. A. Choi, K. S. Nam, and D. M. Woo, "Effects of Phosphorus on Stress of Multi-Stacked Polysilicon Film and Single Crystalline Silicon," *J. Micromech. & Microeng.*, Vol. 9, pp. 252-263, 1999.
- [5] H. Seidel, L. Csepregi, A. Heuberger, and H. Baumgartel, "Anisotropic Etching of Crystalline Silicon in Alkaline Solutions II. Influence of Dopants," *Jour. of The Electrochemical Society*. Vol. 137, Num.11, pp. 3626-3632, 1990.